Switch of fractal properties of DNA in chicken erythrocytes nuclei by mechanical stress

S. V. Grigoriev,[1,2] E. G. Iashina,[1] V. Yu. Bairamukov,[1] V. Pipich,[3] A. Radulescu,[3] M. V. Filatov,[1] R. A. Pantina,[1] and E. Yu. Varfolomeeva[1]

[1]*Petersburg Nuclear Physics Institute, Gatchina, St-Petersburg, 188300, Russia*

[2]*Saint-Petersburg State University, Ulyanovskaya 1, Saint-Petersburg, 198504, Russia*

[3]*Heinz Maier-Leibnitz Zentrum, Lichtenbergstraße 1, 85748 Garching bei München, Germany*

(Received 15 June 2020; accepted 13 September 2020; published 28 September 2020)

The small-angle neutron scattering (SANS) on the chicken erythrocyte nuclei demonstrates the bifractal nature of the chromatin structural organization. Use of the contrast variation (D_2O-H_2O) in SANS measurements reveals the differences in the DNA and protein arrangements inside the chromatin substance. It is the DNA that serves as a framework that constitutes the bifractal behavior showing the mass fractal properties with $D = 2.22$ at a smaller scale and the logarithmic fractal behavior with $D \approx 3$ at a larger scale. The protein spatial organization shows the mass fractal properties with $D \approx 2.34$ throughout the whole nucleus. The borderline between two fractal levels can be significantly shifted toward smaller scales by centrifugation of the nuclei disposed on the dry substrate, since nuclei suffer from mechanical stress transforming them to a disklike shape. The height of this disk measured by atomic force microscopy (AFM) coincides closely with the fractal borderline, thus characterizing two types of the chromatin with the soft (at larger scale) and rigid (at smaller scale) properties. The combined SANS and AFM measurements demonstrate the stress induced switch of the DNA fractal properties from the rigid, but loosely packed, mass fractal to the soft, but densely packed, logarithmic fractal.

DOI: 10.1103/PhysRevE.102.032415

I. INTRODUCTION

Fractal is the self-similar object that repeats its geometrical structure at different scales [1]. One of the most demonstrative objects with fractal dimension $D_F = 2.4$ is a diffusion-limited aggregation (DLA) cluster [2]. A DLA cluster (also known as Brownian tree) is a fractal aggregate, where the shape of the cluster is controlled by the possibility of particles to reach the cluster via Brownian motion. In the living nature the structures are often generated by multiple repetition of the same morphogenetic mechanism, for example, branching. A tree is the most illustrative example of the realization of this mechanism [3,4]. It grows in a way that the sum of squares of the branch's radii on each successive level of branching equals the square of the radius of a preceding branch. The property of recurrence describing the growth of a tree was first noted long ago by da Vinci. Nowadays the fractal concept is one of the most successful ways to describe the living system. It is not a surprise that it has been applied to describe the structural organization of chromatin in the nucleus of a biological cell [5,6].

The model of a crumpled or fractal globule was proposed to describe the three-dimensional configuration of chromatin packaging in a cell nucleus [7,8]. This model explains how a rather long piece of DNA can be reversibly and quickly folded and unpacked when reading the genetic information. The fractal globule is an open macromolecule with hierarchically self-similar packing of the polymer chain. The model suggests that the chromatin fiber is packed in a self-similar manner resembling the Peano curve (space-filling curve) well known in the theory of fractals [1], which has three dimensions and fills the three-dimensional space completely. The reference often made in this concept to the space-filling curves (2D Peano curve and 3D Hilbert curve) is, however, misleading since they are not the fractal objects in the direct sense [1]. Moreover, the most compact packing of the 3D Hilbert curve produces uncountable obstacles for enzymes getting to the specific gene site and thus destroys any accessibility (see arguments in [9,10]).

Obviously to achieve the extreme density of the DNA packing and high accessibility of enzymes to a specific gene site, chromatin cannot be randomly distributed or fully disordered. The oversimplified assumption and expectation to find regular (quasiperiodic) structures in the high order chromatin organization had failed [11]. The chromatin organization appeared to be fractal [12,13] that had required the experimental equipment allowing the study of the chromatin density distribution in the wide spatial range simultaneously. All types of microscopy are much less suited to these purposes as compared with small-angle scattering of neutrons or x rays [14,15]. Even more than that, the chromatin demonstrates a hierarchical structure that includes several organization levels: the organization of chromatin into higher-order domains and the spatial arrangement of chromosomes and genes within the nuclear space [16].

The numerous experiments evidence that the structural organization of chromatin is double scaled with one type of organization in the approximate range from 20 nm to 400 nm, and with another within the range from 400 nm and up to the size of the nucleus of the order of several microns [12,13,17].

Experiments on small-angle neutron scattering show a bifractal structure of the chromatin, confirming the fundamental difference between small-scale and large-scale structures of the chromatin package [18–21].

In their pioneering work of the first decade of the 21st century authors of [18] were able to provide measurements of neutron scattering intensities in chicken erythrocyte nuclei in the range of scattering vectors, covering the entire hierarchy of chromatin structures in a cell nucleus from nucleosomal to the nucleus as a whole. It was found that the exponent of the power function in the cross section of small-angle neutron scattering D equals 2.4 on the scale of 15–400 nm, and it is 2.9 (i.e., close to 3) on the scales from 400 nm to 1500 μm. In the framework of the fractal concept $D = 2.4$ corresponds to the volume (mass) fractal with the fractal dimension $D_m = 2.4$. The exponent close to 3 was recently interpreted as the very special type of fractal organization of matter—the logarithmic fractal [9,21,22]. The SANS and SESANS experiments [21] had shown that the correlation function describing large-scale structure of the chromatin organization in a cell nucleus represents a logarithmic dependence $\gamma(r) \sim \ln(\xi/r)$, i.e., the structure of chromatin forms a logarithmic fractal, which is fundamentally different from the mass or surface fractals.

The neutron scattering technique (with the help of D_2O-H_2O contrasting) was further used to separate the contribution of the DNA architecture that also exhibited two different regimes of fractality with a fractal dimension of $D = 2.2$ in the 15–400 nm spatial range and a $D = 3.2$ exponent for larger length scales [18]. As to the nuclear protein organization, it is found to associate to a fractal behavior with an exponent of 2.5 over the full length spectrum.

As a result, the works in [18–20] have paved the way for detailed studies of the fractal properties of the DNA and protein components as well as the chromatin as a whole. As the obtained results are of great importance we revisited the case of small-angle neutron scattering in the chicken erythrocyte nuclei and repeated the measurements in order to confirm or, perhaps, correct and clarify where it appears to be necessary.

In this study we focus on and answer two questions. How does one identify the two fractal levels of the chromatin differentiated in the SANS experiment? Or, to rephrase, which part of chromatin can one ascribe these fractal properties to? Another question: what are the structures and roles of the DNA and proteins inside the chromatin arrangement on the small-scale and large-scale fractal levels? The combined analysis of the SANS data and atomic force microscopy (AFM) measurements helps to answer the former question giving an evidence for the two types of chromatin with different physical (dense or loose; soft or rigid) and fractal (power function or logarithmic function) properties. By centrifugation of the nuclei disposed on the dry substrate, we were able to apply mechanical stress that transforms nuclei to the disklike shape and, thus, changes their structure, mechanical, and fractal properties. We use the method of the contrast variation in SANS allowing one to measure the partial neutron cross sections to obtain fine details on the role of the DNA and proteins in the construction of the small-scale mass fractal and the large scale logarithmic fractal.

The paper is organized in the following way. Section II represents the description of the sample's preparation and AFM measurements of the chicken erythrocyte nuclei. The experimental data of the SANS measurements using the contrast variation technique are given in Sec. III and Sec. IV for the nondeformed and deformed chicken erythrocyte nuclei, respectively. The discussion and then conclusion are given in Sec. V and Sec. VI.

II. SAMPLES AND ATTESTATION

The samples of isolated chicken erythrocyte nuclei were extracted from the chicken red blood cells. First, the whole blood is centrifuged for 10 min at 170 rcf. The supernatant containing plasma proteins is removed and the resulting precipitate is resuspended in a standard PBS buffer with 6 mM EDTA. Washing procedure is repeated three times. The resulting red blood cells are lysed within 5 min with 0.1% Triton-X100 in culture medium DMEM/F12 with 15 mM Hepes. The obtained erythrocyte nuclei were washed several times in PBS buffer with 3 mM EDTA by centrifugation to completely remove hemoglobin and cytoplasmic proteins. Then nuclei were fixed by 0.5% glutaraldehyde within 10 min and washed from glutaraldehyde by centrifugation. The resulting precipitate was resuspended in PBS. We also centrifuged the part of the nuclei disposed as a thin layer on a glass prior fixation in order to check their resistance to mechanical stress. It turned out that chicken erythrocyte nuclei were flattened in a centrifuge at a speed of 60 rcf.

The process of destruction of cells, separation of the nuclei, and integrity after deformation were controlled by the cytometry. The flow cytofluorimeter (Cell Lab Quanta SC by Beckman Coulter) was used to analyze properties of nuclei. Cell nuclei for analysis performed at a flow cytometer were stained with Hoeghst 33342 (Sigma) fluorescent dye at a concentration of 10 μg/ml. This dye specifically binds exclusively to DNA in its native form along the minor groove. In our research, it is used at saturation concentration. The fluorescence intensity is directly proportional to the amount of DNA in the nucleus. It can be seen from the histograms (Fig. 1) that the fluorescence intensity for all nuclei is the same in both nondeformed and deformed nuclei. Therefore, there is no loss of DNA and its destruction in the used treatments.

The characteristic sizes of the nuclei were investigated using atomic force microscopy on a Solver Bio microscope. Nuclei were deposited on the glass substrate covered by 0.0001% of poly-L-lysine solution, put to the Petri cup, and centrifuged. The glass was extracted and 2 ml of glutaraldehyde were dripped to the surface. After 10 min of incubation the excess of the spacer was rinsed by distilled water and stored overnight.

The morphology of individual chicken erythrocyte nuclei after isolation and different fixation procedures with glutaraldehyde are shown in Figs. 1(a)–1(c). We applied three different procedures to affect the shape of the nucleus: (a) the nuclei were fixed in suspension (glutaraldehyde was added to the vial for fixation) and dropped onto the substrate, then washed; (b) the nuclei were fixed on the substrate (disposed on a substrate and fixed), then washed; (c) the nuclei were disposed on a substrate, first centrifuged (deformed), then fixed and washed.

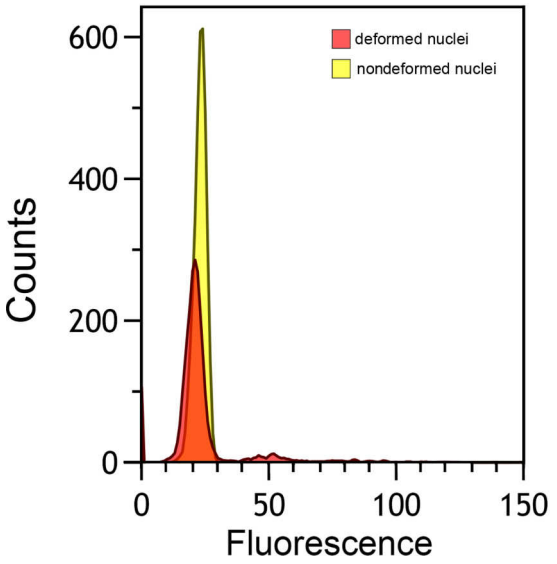

FIG. 1. Flow cytometry histograms for the deformed and nondeformed samples of the chicken erythrocyte nuclei.

We warn the reader that visualization of nuclei in Figs. 2(a) and 2(b) at the first glance taken are somewhat misleading since in reality (not on the picture) the height of the nuclei disposed on the substrate is almost 10 times smaller than its width. Figure 2(a) shows that the nuclei being first fixed in suspension and then disposed on the substrate is squeezed toward the substrate by gravity but still keeps its disklike shape on the substrate plane. Figure 2(b) [as compared to 2(a)] gives an impression on the stability of the nuclei first disposed on the substrate and only then fixed. The gravity squeezes it even more [compared to Fig. 2(a)] toward the substrate. Figure 2(c) shows what happens to the nuclei when not the gravity with 1 g but the centrifuge with tens of g is applied prior to fixation at the substrate. The nuclei are smashed over some aria on the substrate. It is interesting to note that the morphology of the already deformed nuclei could not be further changed in the wide range of applied forces (60–2210 rcf) and different times of centrifugation (5–20 min).

It is instructive to receive the characteristic numbers of the nuclei disposed on the substrate. Figure 3 shows the cross sections of the surface relief of the nuclei shown in Fig. 2 for nuclei fixed in suspension, for nuclei fixed on the substrate, and for nuclei centrifuged and then fixed. Its width exceeds 4 μm but its height is 700 nm for the example of nuclei fixed in suspension, 450 nm for one fixed on the substrate, and 67 nm for one centrifuged and then fixed. The estimated volume of the nuclei decreases upon deformation and is equal to 4.74 μm^3 for the example of nuclei fixed in suspension, 4.14 μm^3 for one fixed on the substrate, and 1.27 μm^3 for one centrifuged and then fixed. Accounting for the integrity of the deformed nuclei, we conclude that the density of material inside the nuclei had increased by a factor of 3.7 upon deformation.

One can conclude that cell nuclei isolated with the help of nonionic detergents are practically devoid of elasticity and, upon sedimentation on a flat surface, form a flat disk-shaped body. At the same time, not all nuclear components are easily

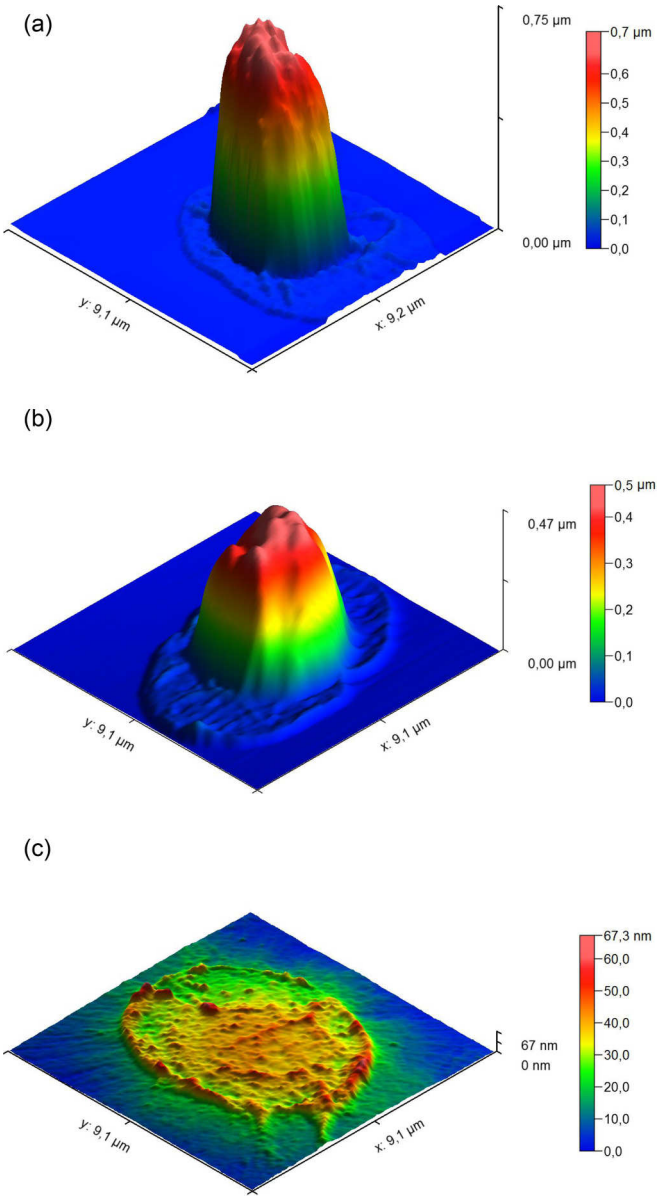

FIG. 2. Surface relief of the chicken erythrocytes nuclei: (a) fixed in suspension, (b) fixed on the substrate, and (c) centrifuged on the substrate and then fixed.

deformed during sedimentation. The nucleus also contains solid formations with the size of 450–700 nm; those are able to resist stress produced by the substrate and the Earth gravity. These relatively solid formations can, nevertheless, be squeezed on the substrate by the stress produced by additional centrifugation of above 60 rcf for a few minutes. They were fixed on the substrate and then can be gently removed from it and dissolved in water for a further study, for example, using small-angle neutron scattering. We are confident that after fixation of nuclei with glutaraldehyde, the strong and rigid covalent bonds are formed in proteins and the nucleus can no longer be destroyed. As was shown by the cytometry, the nuclei transformed to a panlike disk still keep their integrity. As it is shown below, these flattened nuclei can be considered

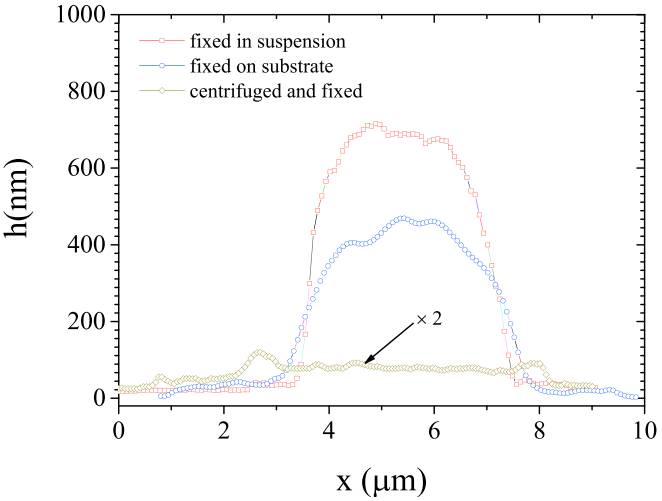

FIG. 3. Cross sections of the surface reliefs of the chicken erythrocytes nuclei shown in Fig. 1 for nuclei fixed in suspension, for nuclei fixed on the substrate, and for nuclei centrifuged (deformed) and then fixed.

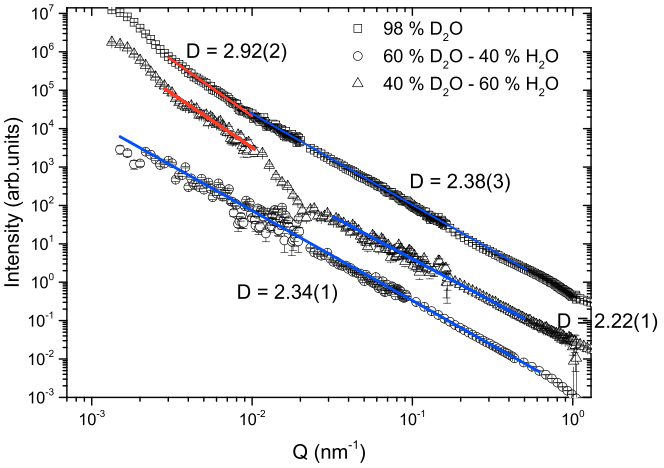

FIG. 4. Small-angle neutron scattering on nuclei of chicken erythrocytes (sample of nuclei fixed in suspension) in heavy water D_2O (chromatin), in 60% D_2O (proteins only), and in 40% D_2O (DNA only).

as rather dense objects whose spatial organization is fully changed as compared to the nondeformed nuclei.

III. TWO-LEVEL FRACTAL ARRANGEMENT OF CHROMATIN IN CHICKEN ERYTHROCYTE NUCLEI

Like the AFM method, the small-angle neutron scattering (SANS) method allows one to determine the characteristic sizes of the nuclei themselves and their internal formations. In addition, SANS also shows whether internal soft matter is homogeneous or contains heterogeneous formations such as nucleoli. Moreover, the SANS provides unique information about changes in density with scale, as happens in fractals.

The structural study of the chromatin in the isolated chicken erythrocytes nuclei was carried out at the KWS-3 instrument in the momentum transfer range 10^{-3}–2×10^{-2} nm^{-1} and at the KWS-2 instrument in the momentum transfer range 10^{-2}–1 nm^{-1} at MLZ, Garching, Germany. Two types of the samples were used for SANS experiments: the sample of nuclei fixed in suspension and the sample of nuclei first dried and deformed (flattened) by centrifugation and then fixed and dissolved in suspension.

In order to study the chromatin arrangement in more detail one has to obtain the partial neutron cross sections of the DNA and protein complexes using contrasting (D_2O and H_2O) techniques. We had performed SANS experiments on the samples diluted in three different D_2O-H_2O mixtures. 100% D_2O was used to get maximal contrast between chromatin and the diluting buffer and to obtain a scattering pattern from all the inhomogeneities of the nuclei. 60% D_2O and 40% H_2O was mixed to match the DNA part of the nucleus and to visualize the protein part only. 40% D_2O and 60% H_2O was prepared to match the protein part and to visualize the DNA part.

Figure 4 shows three scattering curves taken from the chicken erythrocytes diluted in heavy water D_2O (chromatin), in 60% D_2O (proteins only) and in 40% D_2O (DNA only) in the momentum transfer range [10^{-3}–1] nm^{-1}. The two fractal levels are well seen for the scattering curve taken from chromatin (100% D_2O). Exponent D of the power function Q^{-D} is equal to 2.38 ± 0.03 in the Q range [10^{-2}–0.8] nm^{-1} and it is equal to 2.92 ± 0.02 in the Q range [3×10^{-3}–10^{-2}] nm^{-1}. The difference between the indexes observed in different ranges of the momentum transfer Q leads to the conclusion that the fractal structure of the chromatin changes its nature at the transition from small scale (tens and hundreds of nanometers) to larger scale (micrometers).

The exponent 2.38 ± 0.03 reveals the presence of the mass fractal in the Q range [10^{-2}–0.8] nm^{-1} that can be converted to the range from roughly 10 to 600 nm in direct space. The momentum transfer dependence $I(Q) \sim Q^{-3}$ corresponds to the spatial correlation function of the form $\gamma(r) \sim \ln(\xi/r)$ for $\xi < r$ [21], where ξ is the upper boundary of the fractal. Such behavior of the correlation function reveals a special type of fractal object—the logarithmic fractal—in the Q range [3×10^{-3}–10^{2}] nm^{-1} that is converted to the range of 600 nm to 2000 nm in direct space. Thus the value of 600 nm can be taken as the borderline between two different types of fractal behavior.

The use of the contrasting mixtures (D_2O-H_2O) provides one with the partial neutron cross sections obtained from the proteins or DNA (Fig. 4). The curve for proteins shows the power dependence Q^{-D} with $D = 2.34 \pm 0.1$ in the whole range of [3×10^{-3}–0.8] nm^{-1} that corresponds to the mass fractal arrangement of the density distribution.

As for the DNA curve, it demonstrates a clear crossover at $Q = 10^{-2}$ nm^{-1}. In the range of [10^{-2}–0.8] nm^{-1} the curve can be fitted by the power function with $D = 2.22 \pm 0.01$. One concludes that the DNA has as well the mass fractal arrangement on the scale from 10 nm to 600 nm. The curve for the DNA demonstrates very different dependence with $D = 3.05 \pm 0.1$ for the low-Q range of [3×10^{-3}–10^{2}] nm^{-1} that is the signature of scattering on the object with the logarithmic fractal distribution of contrast density.

Yet, the measurements of Fig. 4 reveal clearly the crossover in the Q dependences and give the value of $Q = 10^{-2}$ nm^{-1}

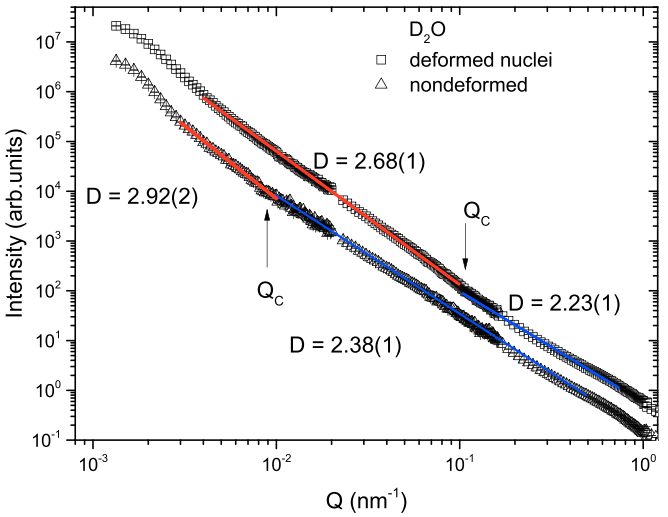

FIG. 5. Small-angle neutron scattering on nuclei of chicken erythrocytes [sample of nuclei deformed (flattened) by centrifugation] in heavy water D_2O (chromatin). The curve for the sample of nuclei fixed in suspension is given in the same picture for comparison.

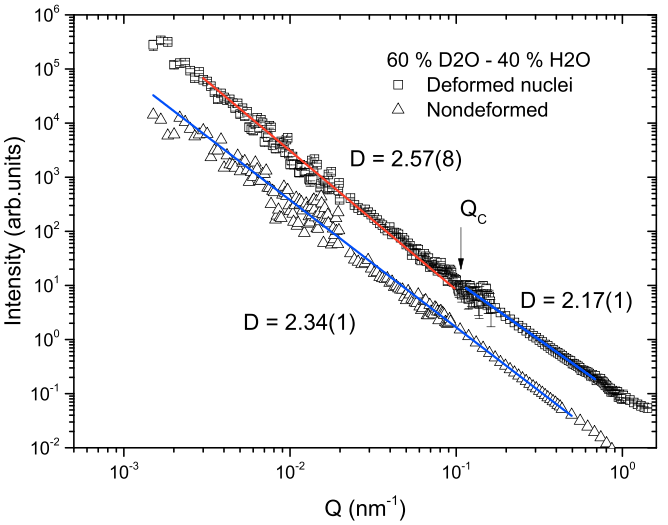

FIG. 6. Small-angle neutron scattering on nuclei of chicken erythrocytes [sample of nuclei deformed (flattened) by centrifugation] in 60% D_2O (proteins only). The curve for the sample of nuclei fixed in suspension is given in the same pictures for comparison.

as the borderline between different fractal arrangement of the DNA as a part and the chromatin as the whole. We correlate this borderline with the size of the solid part of the chromatin obtained in the AFM measurements. We speculate that they are the very same objects inside the nuclei that form the mass fractal arrangement and resist stresses upon sedimentation of nuclei on the substrate. We conclude as well that the nuclei as the whole are soft and the DNA part of the chromatin at this large scale forms the logarithmic fractal while the protein part remains a mass fractal distributed over the whole range of scales. It is important to note that experimental findings shown in Fig. 4 by no means contradict but support the experimental data presented in [18,20,21]. Particularly, the scattering curves taken from the samples used in [18,20,21] and in the present work show the bifractal nature of the chromatin structural organization with the inflection point at $Q_c = 10^{-2}$ nm^{-1}. The obtained fractal dimensions either coincide or are close to each other in all cases.

We note that all data taken for 40% and 98% D_2O (Fig. 4, Fig. 5, and Fig. 7) have an inflection point around 0.003 nm^{-1}. As was shown in [18] the Q dependency of the scattering intensity in the range $Q < 0.003$ nm^{-1} follows the Guinier law with the gyration radius $R_g = 1.1$ μm, that corresponds to the spherical particle diameter of approximately 3 μm, which is close to the size of the chicken erythrocyte nucleus.

IV. SMALL-ANGLE NEUTRON SCATTERING FROM DEFORMED NUCLEI OF CHICKEN ERYTHROCYTES

The sample with deformed nuclei was prepared by centrifugation of the nuclei that resulted in their flattening, i.e., transformation of the spherical nuclei to the panlike disk with a thickness of 67 nm and a diameter of 5.5 microns (Fig. 3). This transformation has dramatic effect on the chromatin organization. The results of the SANS experiments on deformed nuclei are shown in Figs. 5–7.

The scattering curve on deformed nuclei diluted in D_2O is shown in Fig. 5. It has a power-law character with the exponent $D = 2.68 \pm 0.01$ in the range of momentum transfer $[4 \times 10^{-3}$–$10^{-1}]$ nm^{-1}. It has a crossover point at $Q = 10^{-1}$ nm^{-1} to a new fractal regime with $D = 2.23 \pm 0.01$ in the range $[10^{-1}$–$0.8]$ nm^{-1}. The crossover point corresponds to 60 nm, i.e., to the thickness of the flattened nuclei. We plotted the curve for the sample with nondeformed nuclei in the same picture for comparison. The fair comparison shows that these two curves are rather similar in the Q range $[10^{-1}$–$10^{0}]$ nm^{-1} and they deviate at smaller Q.

Scattering curves on both deformed and nondeformed nuclei diluted in the mixture 60% D_2O + 40% H_2O are shown in

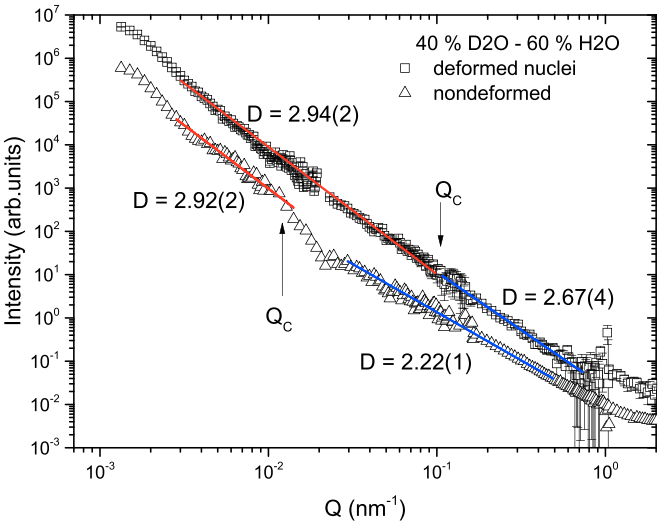

FIG. 7. Small-angle neutron scattering on nuclei of chicken erythrocytes [sample of nuclei deformed (flattened) by centrifugation) in 40% D_2O (DNA only). The curve for the sample of nuclei fixed in suspension is given in the same pictures for comparison.

Fig. 6. This diluting mixture helps to highlight scattering from the proteins. Again they show much similarity in the Q range of [10^{-1}–0.8] nm^{-1} with exponent $D = 2.17 \pm 0.01$ for deformed nuclei and $D = 2.34 \pm 0.01$ for nondeformed nuclei. The two curves differ in the small-Q range: the power law for the deformed nuclei is characterized by $D = 2.57 \pm 0.08$ and one for the nondeformed nuclei follows the dependence with $D = 2.34 \pm 0.1$ in the whole Q range.

The most intriguing results are shown in Fig. 7 for the scattering dependences on both deformed and nondeformed nuclei diluted in the mixture 40% D_2O + 60% H_2O. These scattering curves are originated from the DNA part of the nuclei. Remarkably, the scattering curve associated with the deformed nuclei is described by a power function $I(Q) \sim Q^{-D}$ with the power $D = 2.94 \pm 0.02$ in the momentum transfer range [4×10^{-3}–10^{-1}] nm^{-1}. It has a crossover point at $Q_c = 10^{-1}$ nm^{-1} to a new fractal regime with $D = 2.67 \pm 0.04$ in the range [10^{-1}–10^{0}] nm^{-1}. This curve deviates strongly from the one for nondeformed nuclei. They are similar only in the small-Q range, where the power dependence is close to 3.

We conclude that, first, all three scattering curves from the deformed nuclei have the crossover point at $Q_c = 10^{-1}$ nm^{-1} that corresponds to the thickness of the deformed nuclei in 67 nm. Secondly, the crossover point for the deformed nuclei is shifted by one order toward larger Q as compared to nondeformed nuclei. Thirdly, the crossover points for deformed and nondeformed nuclei being converted to the direct space do coincide with the thickness of the nuclei registered by the AFM technique (Fig. 3).

To further summarize, the borderline between fractal levels can be shifted by mechanical stress applied to the nuclei. The DNA part of the nuclei suffers more from the stresses of changing its state with the fractal dimension $D = 2.2$ to the state with fractal dimension $D = 2.94$ that is close to the logarithmic fractal. The protein part changes its fractal dimension from 2.34 to 2.57 upon deformation, i.e., it is affected by deformation as well, but somewhat less than the DNA, remaining the mass fractal.

This experiment shows that the DNA and proteins should have different structural arrangement being under the same conditions. Probably one may conclude that the structural organization of the DNA can be stable in two different states: the logarithmic fractal with $D \approx 3$ and the mass fractal with $D \approx 2.2$. The protein part can be realized as the mass fractal with $D \approx 2.34$ that may increase to $D \approx 2.57$ in dependence on the state of DNA structural organization.

V. REMARKS and DISCUSSION

(1) We have confirmed the results of the previous studies [18,20,21] demonstrating the bifractal structure of the chromatin organization in the nuclei of the chicken erythrocytes. This bifractal nature of the chromatin is caused by the bifractal DNA arrangement, while the proteins though being fractal play a passive role [18]. The crossover point between two fractal levels is equal to $Q_c = 10^{-2}$ nm^{-1} (600 nm in direct space) in the native conditions of the chicken erythrocyte nuclei. The DNA has a mass fractal arrangement with $D = 2.21 \pm 0.01$ for the smaller scale $Q > Q_c$ and the logarithmic fractal arrangement for the larger scale $Q < Q_c$. The proteins are arranged in the mass fractal with dimension $D = 2.34 \pm 0.01$.

(2) The internal structure of the nuclei can be considerably changed by the mechanical stress resulting in deformation of the nuclei. For the mechanically flattened nuclei the crossover point is shifted to the value of $Q_c = 10^{-1}$ nm^{-1} (60 nm in direct space). The DNA has the logarithmic fractal arrangement for the larger scale $Q < Q_c$ and the mass fractal arrangement with $D = 2.67 \pm 0.01$ for the smaller scale $Q > Q_c$. The proteins are arranged as the mass fractal with dimension that is slightly larger than 2.5.

(3) The objects with large fractal dimensions are characterized by larger internal density [10]: thus the logarithmic fractal is two times more dense as compared to the mass fractal with $D = 2.5$ and four times more dense as compared to the mass fractal with $D = 2.25$. The mechanical stress results in condensation of the matter of nucleus and transformation of DNA from the low density mass fractal with $D = 2.2$ into the high density logarithmic fractal.

(4) This transformation occurs in the jumplike mode from one state to another showing that the crossover points are numbers characterizing the internal structure of the nuclei. In other words, the DNA unit (and therefore chromatin) in the state of the mass fractal will occupy the space of order of $600 \times 600 \times 600$ nm^3, while the DNA unit in the state of the logarithmic fractal will collapse four times in volume and occupy much smaller space.

(5) The height of this disk measured by atomic force microscopy (AFM) coincides closely with the fractal borderline, thus characterizing a type of chromatin at smaller scale as being rigid and one at larger scale as being soft. We correlate the mechanical properties (rigid or soft) obtained from AFM and the fractal properties (loose or dense) obtained from SANS. Combining the results of SANS and AFM measurements one concludes that the chromatin in nuclei is characterized as a rigid, loosely packed, mass fractal at smaller scale and as a soft, densely packed logarithmic fractal at larger scale. The mechanical stress induced by centrifugation switches the DNA fractal properties from the rigid, but loosely packed, mass fractal to the soft, but densely packed, logarithmic fractal that shows the ability of DNA for such transformation. This transformation may occur upon density increase produced in the course of the natural life cycle or by mechanical pressure as it is done above.

VI. CONCLUSION

In this paper we have shown that spatial organization of chromatin in the nucleus of chicken erythrocytes is described by the bifractal model that is originated from the bifractal nature of the DNA large-scale arrangement. The DNA is arranged as a low density mass fractal ($D = 2.2$) for the smaller scale and it is able to condense into the logarithmic fractal at the larger scale. The logarithmic fractal implies a hierarchical branched structure similar to a three-dimensional spherically symmetric tree of folds, which ensures the maximum availability of any section from the outside and the most compact, dense structure. Apparently, such a structure is characteristic for living systems.

We have shown that with the mechanical stress we are able to switch the DNA inside nuclei from the mass fractal state to the logarithmic fractal state. This experiment shows the relation between mechanical and structural properties of the DNA at large scale and paves a way for manipulations of these properties.

ACKNOWLEDGMENTS

We like to thank the neutron center MLZ for the beamtime allocation. This work is supported by the Russian Science Foundation (Grant No. 20-12-00188). The authors also thank A. M. Visloguzova for help with the data treatment.

[1] B. Mandelbrot, *The Fractal Geometry of Nature* (Freeman, New York, 1983).
[2] J. Feder, *Fractals* (Plenum, New York, 1998).
[3] J. O. Indekeu and G. Fleerackers, Physica A **261**, 294 (1998).
[4] C. Eloy, Phys. Rev. Lett. **107**, 258101 (2011).
[5] A. Yu. Grosberg, S. K. Nechaev, and E. I. Shakhnovich, J. Phys. (Paris) **49**, 2095 (1988).
[6] A. Grosberg, Y. Rabin, S. Havlin, and A. Neer, Europhys. Lett. **23**, 373 (1993).
[7] E. Lieberman-Aiden, N. L. van Berkum, L. Williams *et al.*, Science **326**, 289 (2009).
[8] L. A. Mirny, Chromosome Res. **19**, 37 (2011).
[9] E. G. Iashina, M. V. Filatov, R. A. Pantina, E. Yu. Varfolomeeva, W. G. Bouwman, C. P. Duif, D. Honecker, V. Pipich, and S. V. Grigoriev, J. Appl. Crystallogr. **52**, 844 (2019).
[10] E. G. Iashina and S. V. Grigoriev, JETP **129**, 455 (2019).
[11] Y. Joti, T. Hikima, Y. Nishino, F. Kamada, S. Hihara, H. Takata, T. Ishikawa, and K. Maeshima, Nucleus **3**, 404 (2012).
[12] K. Metze, Expert Rev. Mol. Diagn. **13**, 719 (2013).
[13] K. Metze, R. Adam, and J. B. Florindo, Expert Rev. Mol. Diagn. **19**, 299 (2019).
[14] J. E. Martin and A. J. Hurd, J. Appl. Crystallogr. **20**, 61 (1987).
[15] J. Teixeira, J. Appl. Crystallogr. **21**, 781 (1988).
[16] T. Misteli, Cell **128**, 787 (2007).
[17] A. Bancaud, C. Lavelle, S. Huet, and J. Ellenberg, Nucl. Acids Res. **40**, 8783 (2012).
[18] D. V. Lebedev, M. V. Filatov, A. I. Kuklin, A. Kh. Islamov, E. Kentzinger, R. Pantina, B. P. Toperverg, and V. V. Isaev-Ivanov, FEBS Lett. **579**, 1465 (2005).
[19] V. V. Isaev-Ivanov, D. V. Lebedev, H. Lauter, R. A. Pantina, A. I. Kuklin, A. Kh. Islamov, and M. V. Filatov, Phys. Solid State **52**, 1063 (2010).
[20] A. V. Ilatovskiy, D. V. Lebedev, M. V. Filatov, M. G. Petukhov, and V. V. Isaev-Ivanov, J. Phys. Conf. Ser. **351**, 012007 (2012).
[21] E. G. Iashina, E. V. Velichko, M. V. Filatov, W. G. Bouwman, C. P. Duif, A. Brulet, and S. V. Grigoriev, Phys. Rev. E **96**, 012411 (2017).
[22] E. G. Iashina and S. V. Grigoriev, J. Surf. Invest.: X-Ray, Synchrotron Neutron Tech. **11**, 897 (2017).